Proceedings of the Research Institute of Atmospherics,
Nagoya University, vol. 19 (1972)

VLF HISS OBSERVED AT SYOWA STATION, ANTARCTICA - II

Occurrence and Polarization of VLF Hiss During Disturbances

Yoshihito TANAKA

Abstract

The occurrence of VLF hiss is the greatest before the local magnetic midnight. Diurnal variations of occurrence probabilities are remarkably similar in the receiving frequencies of 5, 8, 12, 25 kHz. And they seem to coincide well with the diurnal pattern on the flux intensity of soft electrons ($\sim$1 kev) precipitating over the station. The maximum energy is received near 10 kHz.

There is a positive correlation between the occurrence of VLF hiss and K-index in geomagnetically undisturbed period, but the occurrences decrease during geomagnetic disturbances. The dependence of flux density on geomagnetic activity is also similar to the occurrence of VLF hiss. These facts clearly suggest that VLF hiss is generated in higher altitudes than the auroral ionosphere.

The polarization at 12 kHz is independent of geomagnetic activity and the energy of VLF hiss, and it is roughly constant during a discrete VLF event appearing in geomagnetically undisturbed period. These results seem to suggest that wave couplings do not effectively occur in the lower ionosphere and the energy of VLF hiss is decided by the amount of precipitating soft electrons, and that VLF hiss propagates downward in the field aligned duct to an upper region of the auroral ionosphere.

The distribution of (R/L) values observed is to be reasonably explained by the simultaneous arrival of multiple waves which independently come down with not so large angles of incidence roughly within the magnetic meridian plane.

So, it is concluded that auroral hiss can not propagate to lower latitudes in the earth-ionosphere wave guide because of re-penetration into the auroral ionosphere and the inclination of incident angle toward higher latitude, so that auroral hiss is unique in the auroral zone and it is essentially different from low latitude type VLF hiss.

1. Introduction

Ellis (1959) first observed VLF hiss Camden ($-42°$ geomag. lat.) in Australia and he has found that the large magnetic storm is always accompanied with wide-band VLF noise burst but the noise bursts which are usually in a narrow band centered at around 5 kHz do not relate to the magnetic activity. Dowden (1960, 1962) observed VLF hiss events even at more than 200 kHz during strong geomagnetic disturbances at Hobart in Tasmania. We have found a high correlation between the occurrence of VLF hiss observed at Moshiri (34° geomag. lat.) and the geomagnetic activity measured by magnetic storm and the daily sum of K or K_p indices, and that VLF hiss which is usually in a narrow band centered at 5 kHz generally occurs in the last phase of the storm (Iwai et al. 1964, Tanaka & Kashiwagi 1968).

Martin et al. (1960) investigated VLF hiss observed at Byrd Station ($-70.5°$ geomag. lat.) and indicated an association between VLF hiss and aurora. Helms & Turtle (1964) investigated aurora, magnetic activity, VLF and ELF noise events observed at Byrd Station and have found that the geophysical events can be divided into the following two groups. One group is characterized by the impulsive events near the magnetic midnight and consists of auroral flare-up, hiss burst and irregular type micropulsation (p_i). The other group characterized by regular events near the magnetic noon, consists of polar chorus and continuous type magnetic micropulsation (p_c). Moreover, they have found that when an aurora flares up toward the zenith and then sharply breaks up around the zenith, the aurora is accompanied with a sudden hiss burst, p_i and a sharp and large decrease of magnetic H-component and an impulsive hiss burst occurs almost at the same time and falls in short period before the maximum auroral activity.

Harang & Larsen (1965) observed VLF hiss at Tromsö (67° geomag. lat.) and have found that VLF hiss occurs near the magnetic midnight and has a close correlation to small geomagnetic perturbations and a positive correlation to weak CNA at 28 MHz but a negative correlation to the intense absorption. Morozumi (1965) and Morozumi & Helliwell (1966) divided the polar substorm at Byrd Station into three phases (N-1, N-2 and N-3 phases) and found that the N-1 phase before the magnetic midnight is characterized by diffuse or arc aurora, steady hiss and CNA with a low amplitude, the N-2 phase is to the auroral break-up stage accompanied with impulsive VLF hiss, p_i and CNA with a high level, and the N-3 phase is to the post break-up phase with VLF chorus (1 kHz).

Jörgensen (1968) has indicated that VLF hiss is often observed at 500 kHz at Byrd Station and the maximum energy of auroral hiss is received near 10 kHz at Byrd Station and by the satellite OGO 2. Laaspere et al. (1971) have found that auroral hiss is observed in the frequency range of 20Hz-540kHz on OGO 6 and the

region of maximum intensity of auroral hiss coincides with the region of maximum occurrence of 'burst-type' low energy (~0.7 kev) electrons observed by Hoffman (1971).

Ellis (1960) made directional and spaced observations of VLF hiss events at 5 kHz with goniometer arrangements in Australia and shows that most of VLF noise bursts probably come from the southern auroral zone and some bursts come from virtual sources of quite small areas on the earth surface. Jörgensen (1966) summarized VLF hiss observations from thirteen stations in the both hemispheres and indicated a close association of VLF hiss in the auroral zone to high latitude electron flux and then suggested that VLF hiss was ordinarily generated in the zone of auroral particle precipitation and VLF hiss generated at auroral latitude, propagated to lower latitudes in the earth-ionosphere wave guide because the decrease of the maximum spectral density with decreasing latitude (~10 dB per 1000 km) fitted well with propagation loss in the wave guide mode and no detailed correlation to magnetic activity was found outside auroral zone.

Harang & Hauge (1965) studied the arriving direction of VLF hiss by alternately switching the crossed loop antennas to the preamplifier and investigated the polarization by displaying the pattern on a cathode ray tube, near the northern auroral zone. There was no difference of outputs from both frames, and ordinary broad and irregular VLF bursts showed irregular oscillographic patterns. So, it was suggested that VLF emissions came from all directions in an observing point located within a source of bursts. In some few cases when a sudden, single and sharp burst appeared the oscillographic pattern was different and it was almost circular and the sense of rotation was always in the same direction. In this case, it is assumed that the emission came down vertically along the field line with circular polarization. And it was indicated that direction finding experiments with a simple goniometer arrangement are not effective within a source area.

Iwai & Tanaka (1968) studied the direction and polarization of VLF hiss observed at Moshiri and found that the polarizations were usually linear and so in some cases of high level emissions, direction findings with a goniometer arrangement were effective and the directions were northward.

Simultaneous observations carried out at Byrd and Hallet stations which are 1100 km apart (Helms & Turtle 1964) are thought to confirm in the same way as the observations from three stations in Greenland (Jörgensen 1966) that auroral hiss is rather a local phenomenon because auroral hiss is seldom observed at two locations at the same time. Harang (1968) investigated in detail VLF hisses observed at stations close the northern auroral zone and stations at lower latitudes along N-S chain and has found that auroral hisses occur in the auroral zone in the nighttime only and have a different character from low latitude type VLF hisses occurring in the daytime, and auroral hisses attenuate too much to propagate to lower latitudes in the wave guide mode. Vershinin (1970) observed VLF hiss at stations in Siberia and finds that the changing of direction of magnetic antenna orientation strongly affects the level

of registered signal if the source is not just over the point of observation and the ouptut from the magnetic antenna oriented in geomagnetic N-S is the greatest and that at the appearance of isolated bursts of VLF hiss the signal level is independent of the direction of the antenna axis only if the source of bursts is located over the observation point.

Using the data at Syowa Station, Tanaka et al. (1970) pointed out that the auroral hiss generated in the dark magnetosphere comes down with not so large an angle of incidence and right-handed polarization roughly within the magnetic meridian plane.

The relation of soft electron precipitation into the auroral ionosphere to auroral hiss has been pretty well studied (Gurnett 1966, Jörgensen 1968, Laaspere et at. 1971). While, K-index may be a good measure to know the auroral particle precipitation into the ionosphere on a ground station, considering a close relation of K_p-index to auroral precipitation events (Kuck 1970).

On the other hand, there is a good correlation between CNA at 28 MHz and auroral intensity in the zenith at Alta in Northern Norway and a time lag of usually a few minutes between both events is reported (Holt & Omholt 1962). A close correlation between sporadic E and auroral hiss in Greenland and a time lag of usually about ten minutes of f_0 E_s to the peak time of VLF hiss are found (Jörgensen 1964). So, it is recognized that auroral break-up and impulsive VLF hiss which almost simultaneously occur are followed by large and sharp fluctuations of magnetic H-component and CNA with a time lag.

The existence of the field aligned duct in which VLF hiss is trapped seems to be confirmed by the facts of a strong association between VLF hiss and HF radar echoes from F-region field aligned irregularities at Washington State University (Hower & Gluth 1965) and the detection of electron concentration fluctuations produced by auroral particle precipitation at College, Alaska (Lund et al. 1967) and a large intensity fluctuation of a VLF signal (NAA) received on OGO 2 at auroral latitude (Heyborne 1966).

It is still a popular idea that VLF hiss is generated mainly in the auroral zone and the auroral hiss propagates to lower latitudes in the earth-ionosphere wave guide (Jörgensen 1966). But this idea is doubtful because simultaneous observations in the auroral zone are remarkably difficult and there are many differences between auroral hiss and low latitude type VLF hiss in occurrence time, duration, dependence on geomagnetic activity, frequency spectrum and so on. While, within a source area of VLF hiss such as auroral zone, VLF signals are suggested to come from all directions in the wave guide mode (Harang & Hauge 1965). This suggestion also is to be examined because the interpretation of observational results is not always reasonable.

The main purpose of this part is to solve the above-mentioned two questions through statistical investigations into VLF hiss records observed at Syowa Station in 1968 and calculations on the propagation conditions of VLF waves in the model ionospheres.

2. Occurrence of VLF hiss

Fig. 1 shows the diurnal variations of occurrence probabilities normalized by the maximum occurrence number at 5 kHz. It is seen in the figure that each occurrence number is different but the diurnal variation is similar at each frequency.

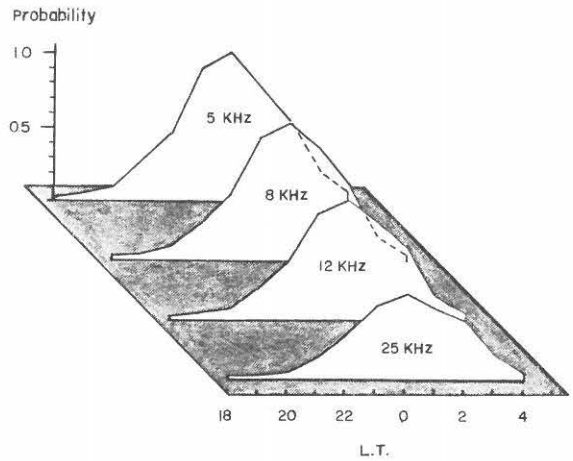

Fig. 1. Local time dependence of the relative occurrence number to the maximum occurrence number at 5 kHz.

The precipitation of auroral particles is shown in Fig. 2 where the triangle represents the precipitation of soft electrons ($\sim$1 kev) and the dot indicates the precipitation of harder electrons ($\geqq$20 kev). Fig. 3 gives the VLF signals (5.5$\sim$8 kHz) observed by the Injun 3 satellite. Fig. 4 shows the zone of maximum occurrence of wide-band hiss (4$\sim$9 kHz). It is found in these figures that the precipitation zone of soft electrons coincides well with the occurrence zones of VLF hisses observed by the satellite and on the ground, except that no VLF hiss is observed on the ground as the precipitating particles are few.

As the result, it is supposed that VLF hiss is generated by soft electrons and that VLF hiss can not propagate from the auroral zone to a distance in the earth-ionoshere wave guide. It is seen in figures 1 and 2 that the occurrence numder has a good correlation to the number of particles precipitating over the observing station.

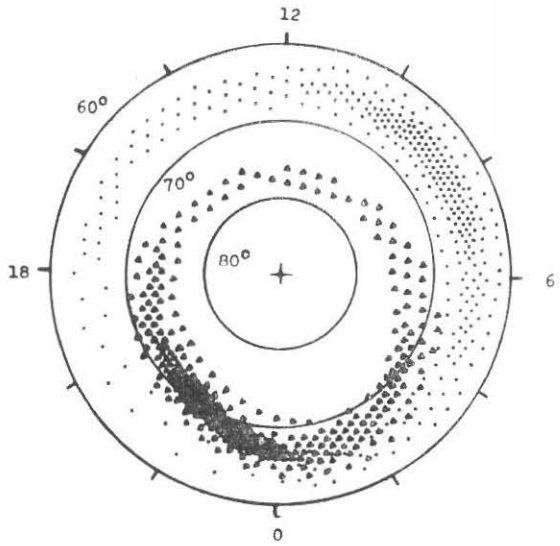

Fig. 2. An idealized representation of the two main zones of auroral particle precipitation in the northern hemisphere, where the average intensity of the influx is indicated very approximately by the density of symbols and the coordinates are geomagnetic latitude and geomagnetic time. The discrete events and the associated splash type precipitation of softer electrons ($\sim$1 kev) are represented by the triangles and the diffuse events together with the drizzle type of harder electrons ($\geq$20kev) precipitation are indicated by the dots. A similar diagram with the two zones shifted poleward by about 5° would be appropriate to the southern hemisphere. (Hartz & Brice 1967)

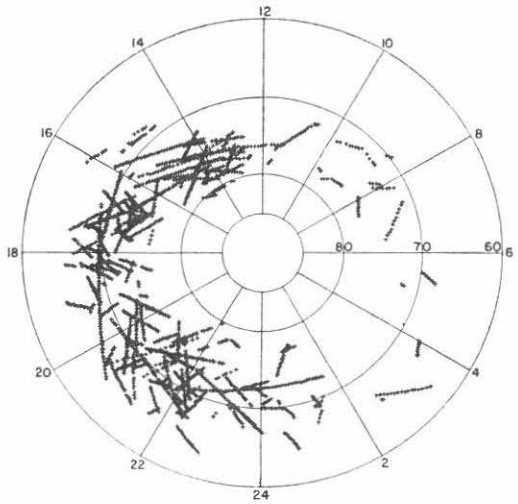

Fig. 3. MLT-INV scatter plot for all points 8 secs. apart with magnetic spectral density exceeding 3×10^{-10} gamma^2 Hz^{-1} from 5.5 to 8.8 kHz. (Gurnett 1966)

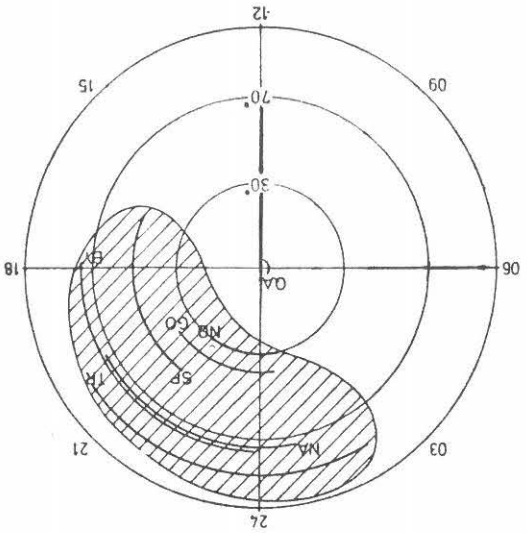

Fig. 4. The hatched area shows the approximate form and location of the zone of maximum occurrence of wide-hand hiss in Mayaud's magnetic coordinate system. The heavy lines indicate in the magnetic time the diurnal occurrence maximums of hiss at various stations at auroral latitudes. (Jörgensen 1966)

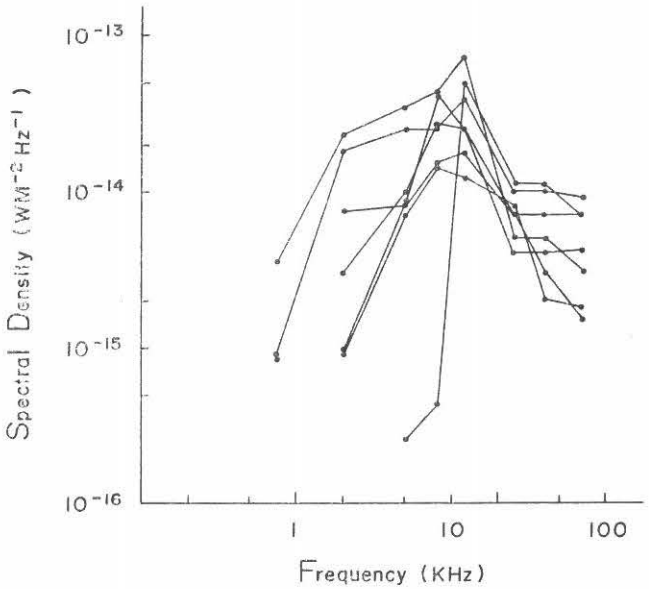

Fig. 5. Frequency spectra of flux density of the peaks in 7 VLF events.

Fig. 5 represents the frequency spectra of the flux density of the peaks in the several events.

Fig. 6 gives the occurrence probability of VLF events as a function of flux density at 5 frequencies. It is seen in figures 5 and 6 that the maximum energy is received near 10 kHz which is consistent with the frequency of maximum intensity in the hiss spectrum theoretically deduced from Cerenkov radiation in the model region of generation in the lower ionosphere by Jörgensen (1968).

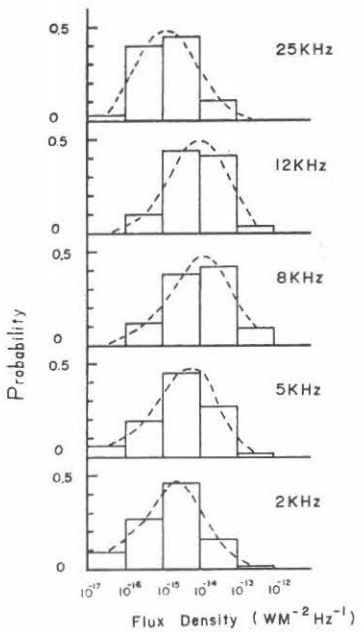

Fig. 6. Occurrence probability of VLF events as a function of flux density at 5 frequencies.

Fig. 7 shows the occurrence probability of VLF hiss at 12 kHz versus K-index, during 21.00-24.00 L. T.. It is found in the figure that the occurrence probability has a positive correlation to the geomagnetic activity in the slightly and moderately geomagnetically disturbed periods and that it decreases during the geomagnetic disturbance. Auroral precipitation events at 10 kev for the entire life of OV3-1 satellite have a good correlation to K_p-indices (Kuck 1970). So, the magnetic disturbance is thought to be caused by the auroral particle precipitation into the ionosphere and the precipitation also simultaneously causes the absorption of VLF hiss. Therefore, it is clear that VLF hiss is generated in higher altitudes than the geomagnetic disturbance. And this is confirmed by the fact that the direction of the pointing flux of VLF hiss was toward the earth in the altitude of 2160 km (Mosier & Gurnett 1969).

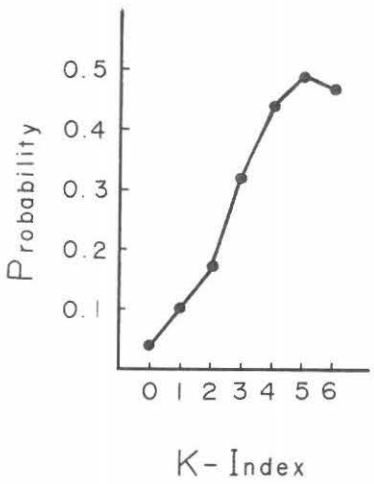

Fig. 7. Occurrence probability of VLF hiss at 12 kHz versus K-index, during 21.00-24.00 L. T.

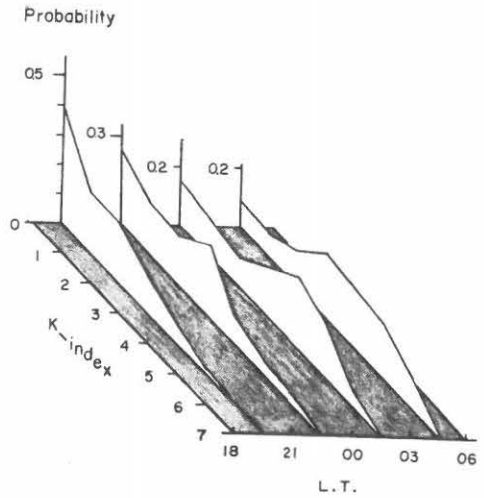

Fig. 8. Local time dependence of K-index.

Fig. 8 gives the local time dependences of K-indices. Moderate geomagnetic disturbances (K-index 3~5) are frequently accompanied with VLF events, as shown in Fig. 7 and their diurnal variations are well related to diurnal variations of the occurrences shown in Fig. 1.

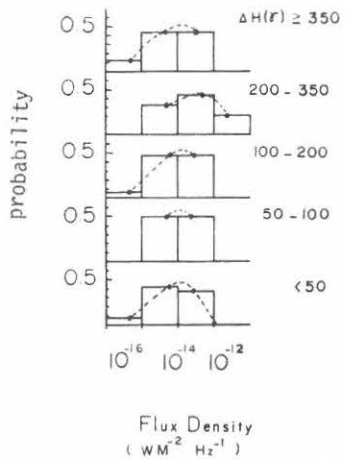

Fig. 9. Occurrence probability of VLF hiss at 12 kHz as a function of flux density.

Fig. 9 shows the occurrence probability of VLF hiss at 12 kHz as a function of flux density for each range of geomagnetic activity. The figure tells that the intensity of VLF hiss increases with the geomagnetic activity but it decreases in the geomagnetically disturbed period for the increase of absorption in the ionosphere.

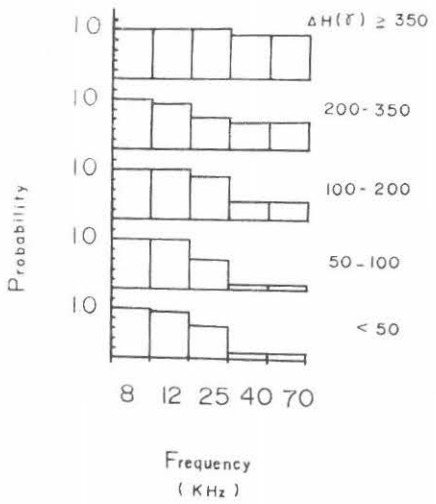

Fig. 10. Occurrence probability of component at each frequency to 5 kHz component in the VLF hiss observed in 1968, for each range of geomagnetic activity.

Fig. 10 gives the occurrence ratio of the component at each frequency to the component at 5 kHz appearing in the VLF events observed in 1968, for each range of geomagnetic activity. It is found in the figure that the frequency range of VLF hiss expands to higher frequency as the geomagnetic activity grows.

Fig. 11 shows the duration of VLF hiss at 12 kHz versus geomagnetic activity. It is shown in the figure that the duration of VLF hiss is longer in slight and moderate geomagnetic disturbances but that it becomes short in geomagnetically disturbed period. And it is generally concluded that a small geomagnetic perturbation associates with steady VLF hiss with lower frequency range and longer period and that at magnetic active phase, VLF hiss is impulsive and its frequency range extends. More active geomagnetic disturbance is associated with the VLF hiss of which frequency range extends more than 100 kHz.

The local time dependence of the relative occurrence rate is similar in the VLF range except the difference of the occurrence number, as shown in Fig. 1. Judging from these facts, the deep precipitation of many auroral particles is thought to generate wide-band VLF hisses, that is, the extension of the frequency range is thought to be related to the spatial extension of the generating region of VLF hiss.

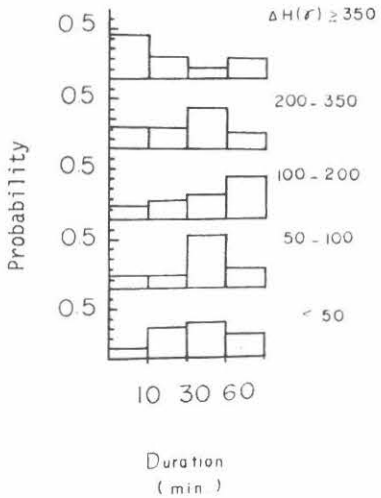

Fig. 11. Duration of VLF hiss at 12 kHz versus geomagnetic activity.

3. Polarization

Fig. 12 shows the ratio of R-component to L-component of VLF hiss at 12 kHz versus K-index, during 21.00-24.00 L. T.. Fig. 13 gives the probability of R/L on VLF events at 12 kHz for 5 ranges of geomagnetic activity. It is found in the two figures that the polarization of VLF hiss is independent of geomagnetic activity.

The precipitation of auroral particles causes the enhancement of ionization in the ionosphere of which lower region is much more ionized. The polarization of VLF hiss is thought to change in the lower region where Q. L. approximation for wave propagation is invalid and wave couplings occur, and the resultant polarization of VLF hiss received on the ground is supposed to be affected. However, the facts shown in the figures teach us that wave couplings do not effectively occur and the actual polarization of VLF hiss does not change markedly in the lower region and therefore the polarization of VLF hiss received on the ground is nearly right-handed circular.

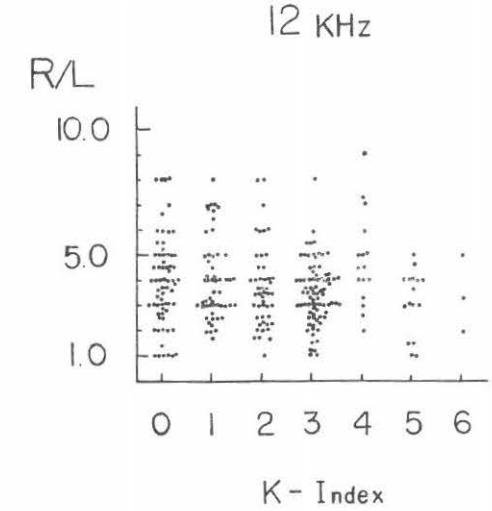

Fig. 12. Ratio of R-component to L-component of VLF hiss at 12 kHz versus K-index, during 21.00-24.00 L. T.

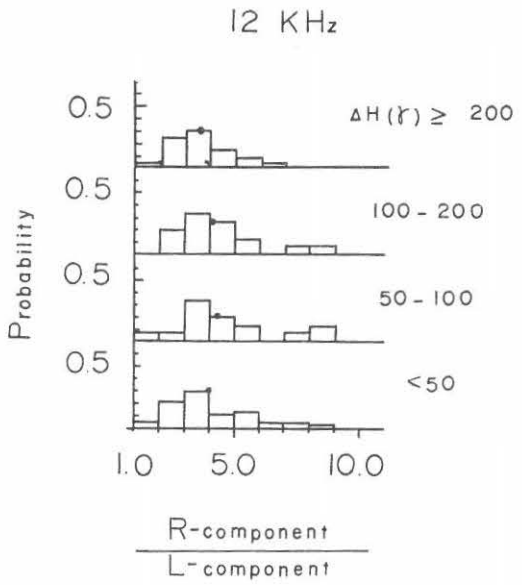

Fig. 13. Probability of R/L of VLF events at 12 kHz, in 5 ranges of geomagnetic activity. A dot represents an average value.

Fig. 14 represents the probability of R/L of VLF hiss at 12 kHz, for each range of flux density. It is found in the figure that the polarization does not relate to the energy of VLF hiss.

Considering that the polarization is not affected through the ionosphere and VLF hiss is generated in higher altitude than auroral altitude and assuming that absorption in the lower ionosphere is roughly constant, the wave normal is thought to be independent of the energy of the hiss generated. Moreover, it is suggested that the energy of hiss is decided not by the energy or energy spectrum of auroral particles but by the amount of auroral particles.

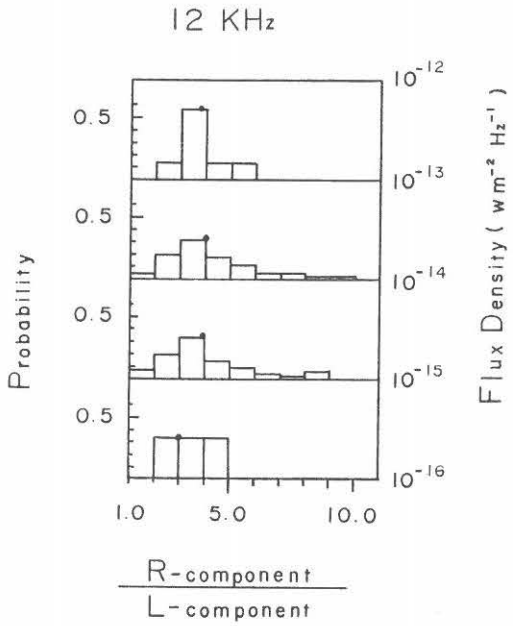

Fig. 14. Probability of R/L of VLF hiss at 12 kHz for each range of flux density. A dot shows an average value.

Fig. 15 shows the ratios of the values of R/L on the sequent peaks to the value of R/L on the first peak in a discrete VLF event which appears in not so much geomagnetically disturbed period with rather a short duration of about ten minutes. In the figure, it is seen that polarizations of the waves sequently received do not change markedly for the period of an event, that is, the wave normals are kept to be almost constant for the period of an event.

Therefore, it is supposed that VLF hiss propagates downward in the field aligned duct to an altitude ($\sim$1000 km) above aurora altitude, considering that although the

auroral ionosphere is disturbed, the condition of the upper ionosphere scarcely changes in the period of an event but the lower region is much more disturbed and the collision frequency of the range is large, so that the field aligned duct can not be formed in the auroral ionosphere except in the upper region.

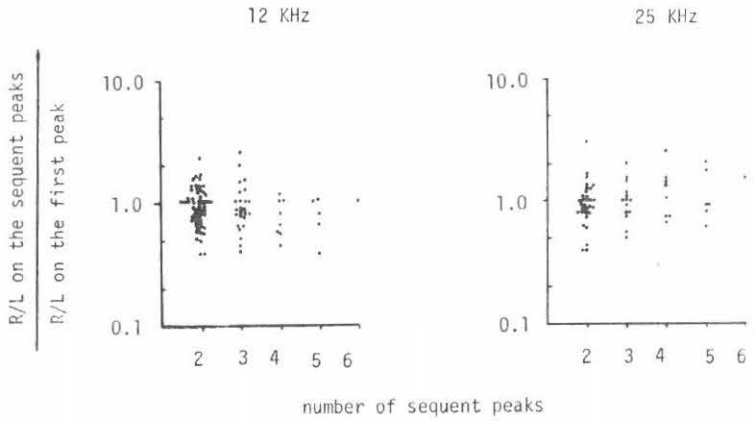

Fig. 15. Ratios of R/L on the sequent peaks to R/L on the first peak in a discrete VLF event appearing in not so much geomagnetically disturded period with rather a short duration of about ten minutes.

4. Discussion

4-1 Effect of wave propagation on polarization

The initial polarization of VLF hiss generated, is thought to be right-handed elliptical in general and then the polarization becomes right-handed circular when the wave propagates in the whistler medium where Q. L. approximation is valid. It is acceptable for the propagation of VLF hiss that the large part of the earth's magnetosphere and ionosphere except the lower part of the ionosphere satisfies the condition for the whistler medium. In the lower region of the ionosphere, Q. L. approximation is invalid. Therefore, a pure ordinary wave (R-wave) travelling downward show a marked change of polarization in the range. As a result, the resultant polarization of VLF hiss received on the ground, is supposed to be affected because of the wave coupling.

In this section, we will first study the changes of polarizations of R-and L-waves travelling downward in this region. So, we would like to take the data of electron

density and collision frequency in the lower range of the auroral ionosphere but to our knowledge, little is known about the auroral ionospheric data. We will use informations obtained by satellites launched at Andöya (geographic lat. 69.2°, long. 16°) in Northern Norway (Jespersen et al. 1966).

Fig. 16 shows the electron density profiles and a collision frequency profile versus height. In the figure, we adopt the electron density which was obtained by the satellite F VIII at 0 dB absorption dip on the riometer of 28 MHz as a calm ionospheric density. And we take the electron density which was observed by the satellite F VII at 0.8 dB absorption dip on the riometer as a representative density of the ionosphere through which VLF hiss is often observed on the ground.

The earth's magnetic field causes the ionosphere to be anisotropic. Hence, there are in general two values for refractive indices, corresponding to the two characteristic waves that can propagate. In a homogeneous medium, the z-axis is chosen in the direction of the wave normal and x- and z-axes are chosen so that the earth's magnetic field lies in the x-z plane as shown in Fig. 17.

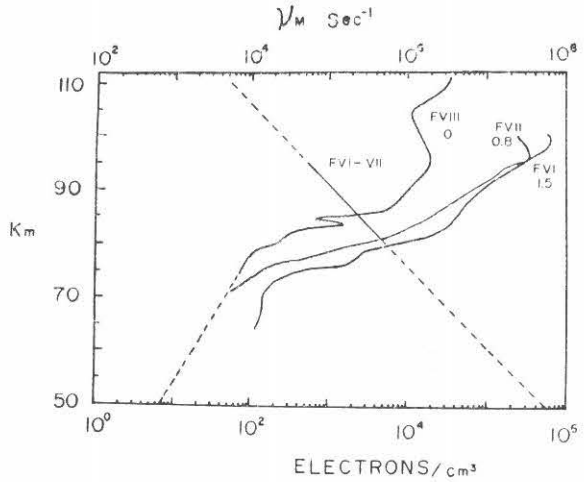

Fig. 16. Electron density profiles and collision frequency observations during auroral absorption events. The results marked F VI and F VII are the night time results on Mar. 1964 and F VIII shows the result measured about 1.5 hrs. before sunset on Mar. 1964. The riometer absorptions were 1.5, 0.8 and 0 dB at 27.6 MHz. The results have been obtained in research rockets fired from Andöya in Northern Norway. Dotted lines are presumably drawn.

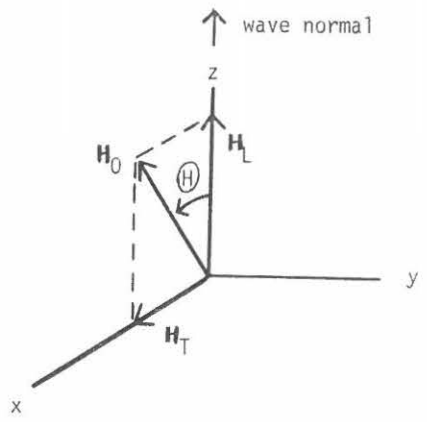

Fig. 17. Wave coordinates in relation to the earth's magnetic field.

The square of the refractive index is given by

$$N^2 = 1 - \frac{X}{U + i Y_L R} \qquad \cdots\cdots (1)$$

and the wave polarization is given by

$$R = \frac{E_y}{E_x} = \frac{i Y_T^2}{2Y_L(1 - X - iZ)} \pm i \left\{ \frac{Y_T^4}{4Y_L^2(1 - X - iZ)} + 1 \right\}^{1/2} \cdots\cdots (2)$$

where,

N = complex refractive index = $\mu - i\chi$

μ = refractive index

χ = absorption index

$X = f_0^2/f^2$ $\quad$ f_0 = electron plasma frequency

$\mathbf{Y} = e\mathbf{B}_0/(mw)$ $\quad$ f_H = electron gyrofrequency

$Y = f_H/f$ $\quad$ m = mass of electron

$Z = \nu/w$ $\quad$ Y = magnitude of $\mathbf{Y}$

$U = 1 - iZ$ $\quad$ Y_L = longitudinal component of $\mathbf{Y}$

l, m, n : direction cosines of $\mathbf{Y}$ $\quad$ Y_T = transverse component of $\mathbf{Y}$

$\mathbf{B}_0$ = magnetic induction of the earth's magnetic field

ν = frequency of collision of electrons with neutral heavy particles

Θ = angle between the earth's magnetic field and wave normal

We are discussing the problems on the propagation and penetration of VLF hiss in the polar ionosphere. So, we will discuss the following two cases for the simplicity of numerical studies.

(1) : Vertical incidence into the free space through the ionosphere. The angle between the earth's magnetic field and vertical direction is 10°32′, corresponding to the line of force at −69.6° geomagnetic latitude.

(2) : Oblique incidence. The earth's magnetic field is vertically upward.

Then, we assume that the ionosphere consists of a number of thin layers horizontally stratified and each layer is sharply bounded homogeneous medium and that the gyrofrequency is constant in the ionospheric region discussed and it is 1.602 MHz, corresponding to the value at 100 km height above Syowa Station.

For the discussion on a wave at an oblique angle of incidence into the free space, we will use the "Booker quartic" equation. Cartesian axes are used with the z-axis vertically upward and the wave normal of the incident wave is in the x-z plane. We assume the earth's magnetic field to be vertically upward. So, the direction cosines of $\mathbf{Y}$ are (0, 0, −1).

Snell's law must be held at each boundary, so that

$$\sin\theta_1 = N \cdot \sin\theta$$

where, θ_1 is the angle between the vertical and the wave normal of an incident wave into the free space. θ is the angle between the vertical and the wave normal of each of downcoming waves in the media.

Now let

$$q = N \cdot \cos\theta$$

q is one root of the Booker quartic equation.

then,

$$N^2 = q^2 + \sin^2\theta_I$$

$$Y_L = -Y \cdot \cos\theta = -Yq\,(q^2 + \sin^2\theta_I)^{-1/2}$$

We solve the quartic equation and we must choose two downcoming waves decided on the condition that imaginary part of q is positive.

Fig.18 shows the refractive indices of the ordinary and extraordinary waves downcoming vertically and obliquely. In the figure, it is found that only ordinary (whistler) mode wave with right-handed polarization can propagate at high altitude.

Fig. 19 gives the polarizations of the two mode waves. Intense coupling which causes coupling echo is expected to occur when $\mu_0 \simeq \mu_X$, $R_0 \simeq R_X \simeq 1$. In the figure, it is suggested that the intense coupling does not occur for VLF range in the lower region of the ionosphere and therefore VLF hiss propagates downward with a pure ordinary mode through the ionosphere.

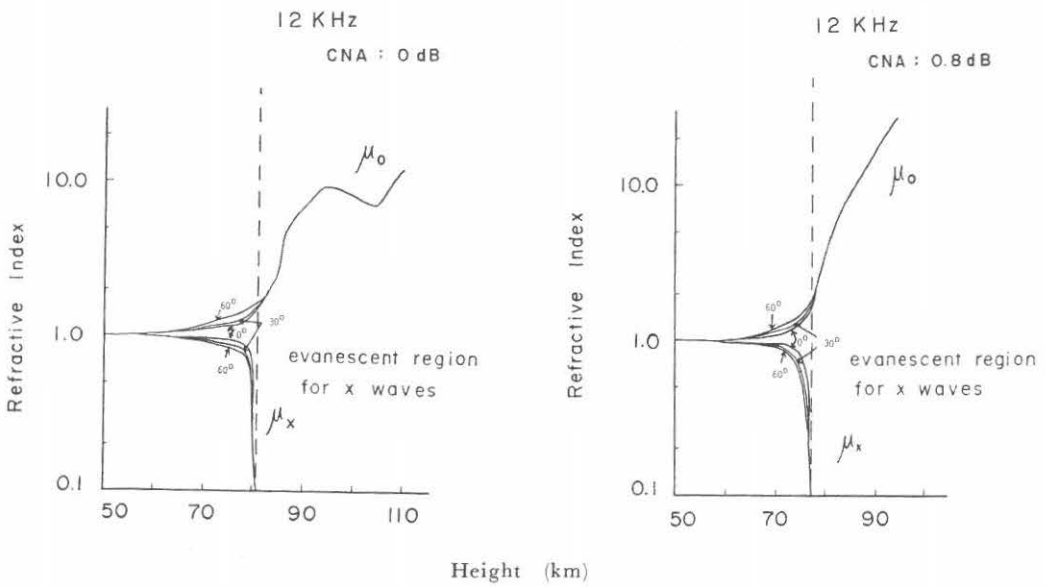

Fig. 18. Refractive indices (μ) of ordinary and extraordinary waves at 12 kHz, vertically and obliquely downcoming in the model ionospheres. 0° corresponds to the vertical incidence ($\theta_I = 180°$). 30°, 60° represent that $\theta_I = 180° \pm 30°$ and $180° \pm 60°$, respectively.

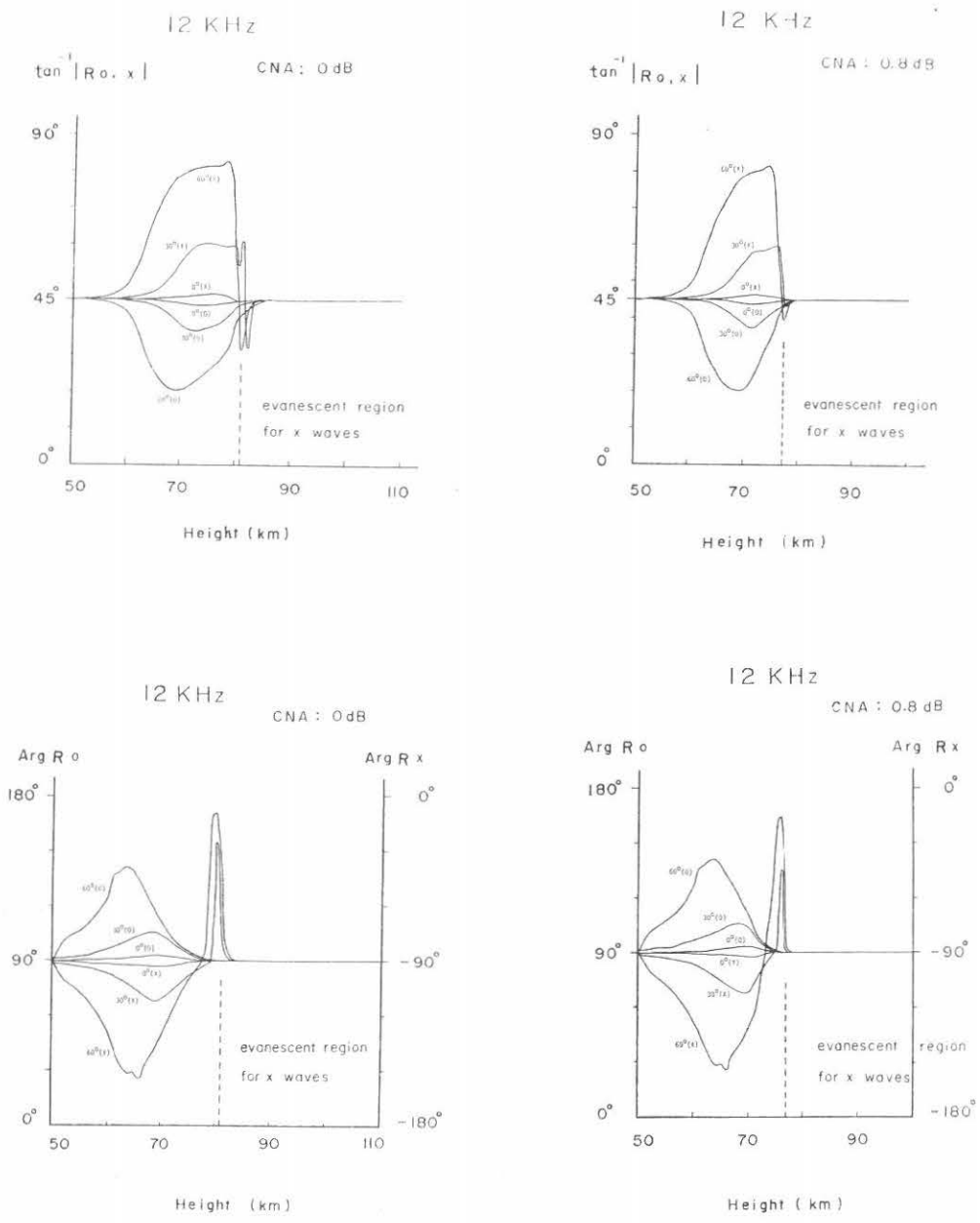

Fig. 19. Polarizations of ordinary and extraordinary waves downcoming through the model ionospheres.

4-2 *Effect of wave coupling on polarization (limiting polarization)*

When a pure ordinary wave travels down within the height range between several tens km and about 100 km where electron density is small but electron collision frequency is large, the wave would show a marked change of polarization in this range. But clearly the actual polarization could not change, since the medium behaves just like the free space. Here the assumption that a characteristic wave retains its correct polarization given by equation (2), must fail.

Consider a characteristic wave travelling down through the lower ionosphere into the free space below. The other characteristic wave is generated by coupling and the coupling parameter Ψ is extremely small and in the small height range the amount of the other characteristic wave generated by coupling is also small. But the two refractive indices N_0, N_x are both nearly equal to unity, so that the two waves travel with the same phase velocity. So, the coupling is cumulative although it is small, so that the amount of the coupling is just enough to keep the polarization constant. Thus, X and Ψ are both very small in the "limiting region".

Now we will discuss whether the coupling in the limiting region occurs effectively in VLF range or not. Firstly, we will study the wave coupling in the limiting region for vertical incidence and then discuss the coupling for oblique incidence when the earth's magnetic field is vertical. Cartesian coordinates are again used with the z-axis directed vertically upward, so that the electron density and collision frequency are functions only of z.

(1) The first order coupled equations for vertical incidence

We may choose the earth's magnetic meridian to be in the x-z plane. In the limiting region, upgoing waves are thought to propagate independently of downcoming waves. So, the first order coupled equations for downcoming waves are given by

$$\left.\begin{aligned} f_2' - i N_0 f_2 &= \Psi f_4 \\ f_4' - i N_x f_4 &= i \Psi f_2 \end{aligned}\right\} \quad \cdots\cdots (3)$$

where, f_2, f_4 which are dependent variables given by Clemmow & Heading (1954), refer to the downcoming ordinary and extraordinary waves, respectively. A prime denotes (1/k) (d/dz). k is propagation constant of the free space. The coupling parameter Ψ is given by

$$\Psi = \frac{R_0'}{R_0^2 - 1} \quad \cdots\cdots (4)$$

Consider an ordinary wave travelling down through the lower ionosphere into the free space. Then, the following results are demonstrated by Budden (1961).

The limiting region is where

$$\left| \frac{1}{4}\left(N_0 - N_x\right)^2 - \frac{1}{2}\,i\left(N_0 - N_x\right)' \right| \simeq \left| \Psi^2 \right| \quad \cdots\cdots (5)$$

Above the limiting region, Ψ^2 is negligible and $f_4/f_2 = 0$, which is correct for a downcoming pure ordinary wave. Below the limiting region, $(N_0 - N_x)$ is negligible and the wave below the region has the constant polarization given by

$$R' = \frac{E_y - E_x}{E_y + E_x} = (a/b)\,\frac{R_L - 1}{R_L + 1} \quad \cdots\cdots (6)$$

where, R' is the polarization referred to new axes formed by a rotation of 45° about the z-axis and R_L is the value of R_0 at the level of the lower limit of the limiting region. a and b are constants which are to be found from initial condition.

(2) The first order coupled equations for oblique incidence when the earth's magnetic field is vertical.

The first order coupled equations for downcoming waves at oblique incidence, are given by

$$\left.\begin{aligned} f_2' - i\,q_0\,f_2 &= -\Gamma_{42}\,f_4 \\ f_4' - i\,q_x\,f_4 &= \Gamma_{42}\,f_2 \end{aligned}\right\} \quad \cdots\cdots (7)$$

where, q_0, q_x are the roots of the Booker quartic equation for downcoming ordinary and extraordinary waves, respectively.

Coupling parameter Γ_{42} is given by

$$\Gamma_{42} = \frac{1}{2}\,\xi\left(q_0 - q_x\right)\left(q_0\,q_x\right)^{-1/2} + \frac{1}{2}\,i\Psi\left(q_0 + q_x\right)\left(q_0\,q_x\right)^{-1/2} \quad \cdots\cdots (8)$$

and

$$\xi = \frac{1}{2}\left(R_0 - R_x\right)^{-1}\frac{1}{k}\,\frac{d}{dz}\log\left\{\frac{U\cos^2\theta_1 - X}{U - X}\right\}$$

R_0, R_x are the roots of

$$R^2 + R\,\frac{i\,Y\sin^2\theta_1}{\{(U-X)\,(U\cos^2\theta_1 - X)\}^{1/2}} + 1 = 0$$

We will apply the study for vertical incidence to the case of oblique incidence. So, the limiting region is where

$$\left| \frac{1}{4}\left(q_0 - q_x\right)^2 - \frac{1}{2} i \left(q_0 - q_x\right)' \right| \simeq \left| \Gamma_{42}{}^2 \right| \quad \cdots\cdots\cdots\cdots\cdots\cdots\cdots\cdots\cdots\cdots (9)$$

Above the limiting region, $\Gamma_{42}{}^2$ is negligible and it can be verified that only a pure ordinary wave propagates downward. Below the limiting region, $(q_0 - q_x)$ is negligible and it can be verified that the wave keeps the polarization constant. In the limiting region, it may be permissible to take $q_0 \simeq q_x \simeq \cos\theta_1$. Then, the polarization of the resultant wave below the ionosphere is also given by the same equation as equation (6) for vertical incidence.

Fig. 20 shows the coupling parameters given by equations (4) & (8), in the model ionospheres. It is seen in the figure that intense couplings do not occur in the lower ionosphere. So, VLF hiss is thought to propagate downward with a pure ordinary mode in the ionosphere above the limiting region.

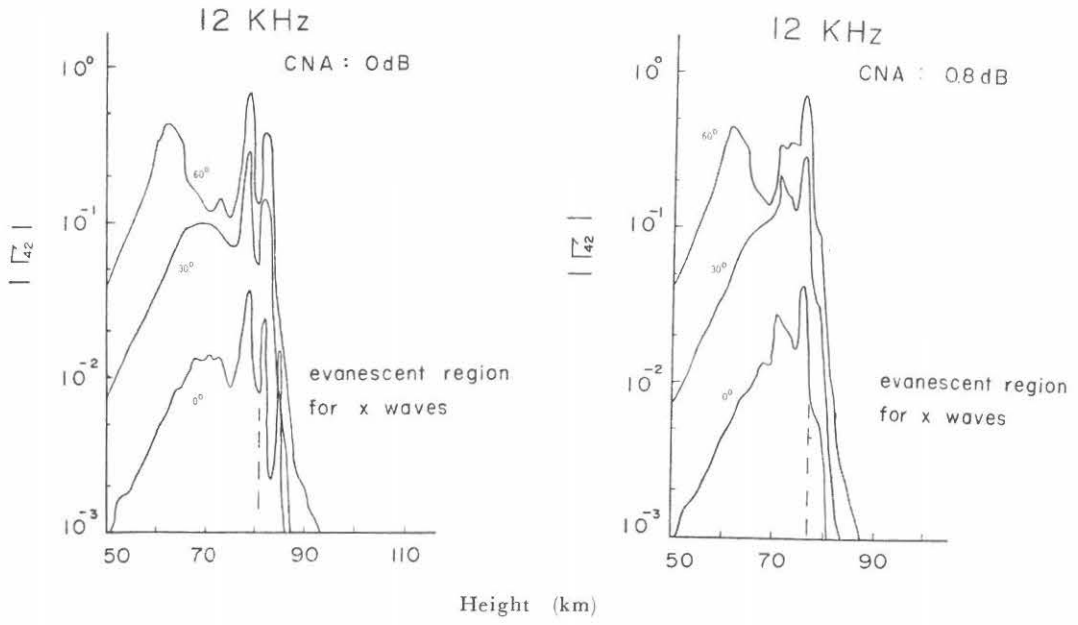

Fig. 20. Coupling parameters $|\Psi|$ for vertical incidence and $|\Gamma_{42}|$ for oblique incidence at 12 kHz in the model ionospheres.

We will calculate the right and left hand sides of equations (5) & (9) at 12 kHz in the model ionospheres. The results calculated are shown in Fig. 21. The curves labelled as 1 in the figure are to the right hand sides, corresponding to the coupling

factors. The curves labelled as 2 are to the left hand sides, corresponding to the differences of phase velocities. We may distinguish the limiting region on the condition that the values of both sides are in the same order of magnitude. It is found in the figure that the limiting region is below the height shown by a broken line for an oblique incidence ($\theta_I = 180° \pm 60°$).

We may take the initial condition that the magnitude of the extraordinary wave is zero in the small range about the upper limit of the limiting region in order to decide (a/b) given in equation (6).
So,

$$(a/b) \simeq 1, \quad \text{for an oblique incidence } (\theta_I = 180° \pm 60°)$$

The polarization (R_I) at the lower limit is found to be right-handed circular in Fig. 19.

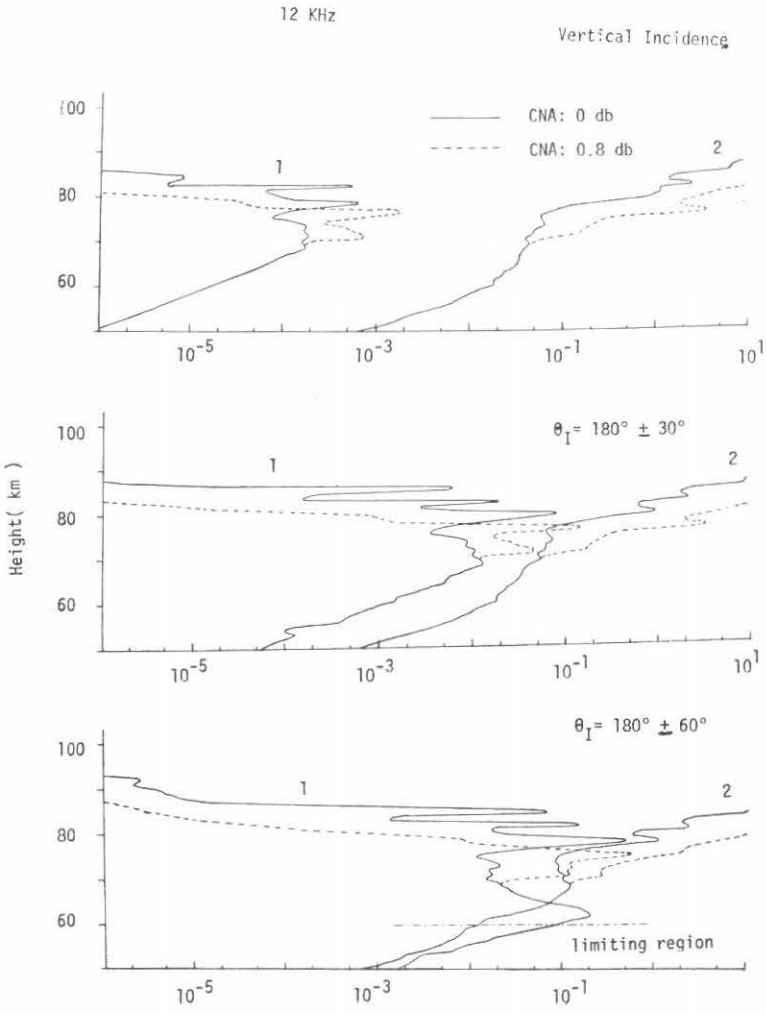

Fig. 21. Right and left hand sides of equations (5) & (9) at 12 kHz in the model ionospheres are shown. Curves labelled as 1 correspond to the right hand sides and curves labelled as 2 correspond to the left hand sides. The limiting region is bounded by a broken line for an oblique incidence.

Therefore, the resultant wave has a right-handed circular polarization. And it is concluded that the coupling in the limiting region is not effective for VLF range because of the long wave length relative to the scale of the region. Hence, VLF hiss downcoming through the ionosphere in whistler mode reaches the ground with right-handed and nearly circular polarization.

4-3 Effect of waves from multiple directions on polarization records

When a single wave with right-handed circular polarization is received, the ratio of R-component to L-component can be given by equation (1) in part I.
And

when	i =	0° ,	R/L = infinite
		10° ,	130.6
		20° ,	32.2
		30° ,	13.9
		60° ,	3.0
		90° ,	1.0

On the other hand, impulsive VLF hiss with wide band frequency range is closely associated with the auroral break-up around the zenith and moreover the results observed with the CRT method show that the incident angles are not so large. When we would explain the observed results on the (R/L) values shown in Fig. 19 in part I under the condition that a single wave with right-handed circular polarization is received, incident angles must be so large in general. This is contrary to the facts mentioned above.

If the incident angle is large, the transmission coefficient of the ionosphere is too small, referring to the numerical results given by Pitteway & Jespersen (1966) with full wave theory. Furthermore, the reflection coefficient is so large that the VLF hiss once penetrating through the ionosphere would propagate to lower latitudes in the earth-ionosphere wave guide. This is contrary to our suggestion that the incident angle of VLF hiss in the auroral zone is not so large and so VLF hiss can not propagate to lower latitudes because of re-penetration into the ionosphere (Tanaka et al. 1970).

Now we, therefore, consider the waves with right-handed circular polarization coming from multiple directions. For the simplicity of numerical studies, we may assume that multiple waves with right-handed circular polarization are simultaneously received with equal magnitude of intensity. Then, the ratio of R-component to L-component of the received signal is given by

$$(R/L) = \left[\frac{\{\sum \cos i_n \sin(\theta_n - \alpha_n) + \sum \sin(\theta_n - \alpha_n)\}^2 + \{\sum \cos i_n \cos(\theta_n - \alpha_n) + \sum \cos(\theta_n - \alpha_n)\}^2}{\{-\sum \cos i_n \sin(\theta_n + \alpha_n) + \sum \sin(\theta_n + \alpha_n)\}^2 + \{\sum \cos i_n \cos(\theta_n + \alpha_n) - \sum \cos(\theta_n + \alpha_n)\}^2} \right]^{1/2} \quad (10)$$

where, θ_n is the azimuthal angle of n-th wave, measured clockwise from the geographic north. i_n is the incident angle of n-th wave and α_n is the phase difference given by $wt_n = wt + \alpha_n$.

Appling Fermat's principle to the plane ionosphere, Maeda & Kimura (1956) have demonstrated that the wave radiated in every direction into the lower ionosphere is focussed into the magnetic meridian plane as it reaches the top of F layer. VLF hiss of which energy is radiated along cones about the magnetic field line because of the symmetry of the medium, can be supposed to be focussed into the magnetic meridian plane by appling their result to VLF hiss propagating downward through the magnetosphere. When VLF hiss is received, the ionosphere is moderately disturbed. So, it can be also supposed that the energy of VLF hiss focussed is somewhat scattered out of the magnetic meridian plane by the irregularities in the auroral ionosphere.

Now, we will discuss two and three waves with right-handed circular polarization and with equal intensity. Then, we assume that the incident angle of each wave is different and the azimuthal angle is different or equal and that the phase of each wave is not related mutually and in other words, the phase is distributed completely at random.

How are the (R/L) values distributed when the assumption is satisfied? Fig. 22 gives the distribution of (R/L) for the received signal in the time when the waves are simultaneously received under the following conditions, in the numerical analysis with equation (10).

(1) Two waves are simultaneously received.

Incident angles: 30°, 50°; 40°, 60° or 50°, 70°

Azimuthal angles:

0°; corresponding to two waves coming from geomagnetic north

−15°∼15°; corresponding to two waves coming from arbitrary directions within −15°∼15° about geomagnetic north.

−30°∼30°; corresponding to two waves coming from arbitrary directions within −30°∼30° about geomagnetic north.

all directions; corresponding to two waves with arbitrary angles of azimuth.

(2) Three waves are simultaneoussly received.

Incident angles; 30°, 40°, 50°; 40°, 50°, 60° or 50°, 60°, 70°

As for azimuthal angles, the condition is similar to that for two waves.

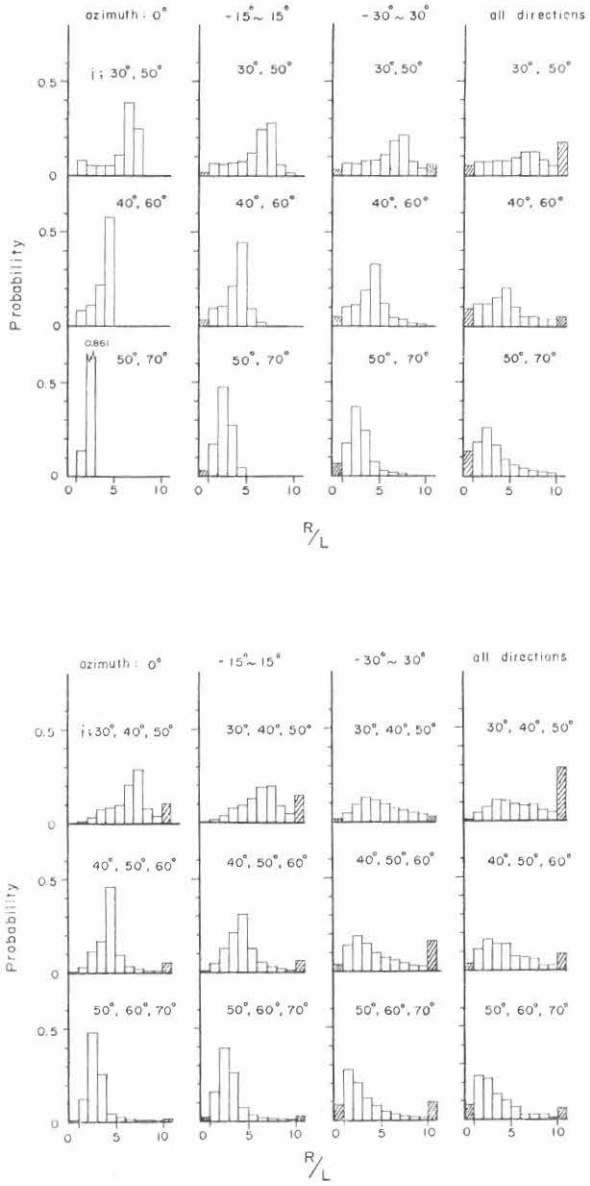

Fig. 22. Distributions of (R/L) values in the times when two and three waves with right-handed circular polarization and with equal amplitude are simultaneously received. The phase of each wave is arbitrary and distributed completely at random. The hatched regions represent the distribution probabilities for (R/L) less than 1.0 and greater than or equal to 10.0.

On the other hand, we can find immediately in equation (10) that if some waves with equal angle of incidence are received at the same time, (R/L) value is equal to that for a single wave. Judging from this fact and the observed result on (R/L), it may not be recognized that some waves with equal angle of incidence are usually simultaneously received. And it can be easily seen in the equation that if a number of waves with equal angle of azimuth (for example, waves from geomagnetic north) are simultaneously received with phases distributed at random, (R/L) value is 1.0 or near 1.0.

It it suggested in the figure that the distributions for two or three waves coming with not so large angles of incidence from the directions within small angles about the geomagnetic north are roughly similar to the observed results on (R/L) values shown in Fig. 19 of part I and that the distributions for the waves coming from arbitrary directions do not coincide at all with the observed results. Therefore, VLF hiss is thought to propapate downward with not so large an angle of incidence roughly in the magnetic meridian plane through the ionosphere into the free space and to reach the ground.

However, a little difference on the distributions of (R/L) values between the observation and our model, may be caused by the simplicity or a little inadequancy of our model. (R/L) values of less than 1.0 and greater than or equal to 10.0 shown in the figure by hatched regions, are given by equation (10) on the condition that the phase differences are large and the waves are almost in anti-phase. Whereas, the intensity of the received signal under the condition becomes, in practical observation, too small to be detectable.

In the present time, we can not explain reasonably the slight difference on (R/L) values observed between 12 and 25 kHz.

Harang & Hauge (1965) and Harang (1968) indicated that VLF hisses were received without directional properties through alternative switching of N-S and E-W loop antennas and that VLF bursts ordinarily showed irregular oscillographic patterns. They suggested that VLF signals came from all directions. Their suggestion is apparently not consistent with our suggestion. However, their suggestion is thought to be not always correct, because VLF hiss is supposed to propagate downward with a small incident angle and with right-handed and nearly circular polarization.

Vershinin (1970) observed VLF hiss at stations in Siberia and finds that the changing of direction of magnetic antenna orientation strongly affects the level of registered signal if the source is not just over the point of observation and the output from the magnetic antenna oriented in the geomagnetic N-S is the greatest and that at appearance of isolated bursts of VLF hiss the signal level is independent of the direction of antenna axis only if the source of bursts is located over the observation point. This fact seems to confirm our suggestion.

4-4 Incident angle and direction

In order to investigate the angle between the wave normal and the earth's magnetic field within the ionosphere, we will again use the Booker quartic equation. Cartesian axes are used with the z-axis vertically upward and the incident wave is in the x-z plane. Within the ionosphere, the cosine of the angle between the wave normal and the vector **Y** is

$$(l \sin\theta_1 + q\, n)\,(q^2 + \sin^2\theta_1)^{-1/2}$$

q is generally complex, so that the direction cosine of the wave normal is complex. The wave of this kind is called as the "inhomogeneous plane wave" discussed by Budden (1961). But the imaginary part is usually negligible in the practical ionosphere. Now, the angle between the earth's magnetic field and the vertical is assumed to be 10°32′, corresponding to the angle at −69.6° geomagnetic latitude.
Hence,

$$l = -(\sin 10^\circ 32') \cos\gamma, \quad n = -\cos 10^\circ 32'$$

where, γ is the angle between the earth's magnetic meridian plane and the incident plane.

Fig. 23 represents the angle between the wave normal and the vector **Y** against the incident angle into the free space for the wave at 12 kHz propagating downward within the plane at a certain angle (γ) to the magnetic meridian plane. Here, it is assumed that the electron density is 2×10^3 cm^{-3} and the collision frequency is negligibly small and the gyrofrequency is 1.08 MHz, corresponding to the value at 1000 km height along −69.6° geomagnetic line of force.

Lund et al. (1967) compared Explore 20 topside electron number density data with simultaneous auroral backscatter data obtained at College, Alaska and have shown that auroral precipitation produces electron concentration fluctuations that are large in amplitude (of the order of 2 to 5 times ambient) and small in geographic size (of order 1-10 km), along with a general increase in the ionospheric electron numder density within the latitudinal region containing the precipitation, at all altitudes between the F-layer maximum and the height of the satellite (about 1000 km).

Heyborne (1966) showed by means of the OGO 2 satellite that noise at 17.8 KHz (NAA) was regularly observed at auroral latitude and very often the noise amplitude changed by more than 40 dB, while the satellite was moving only a few degrees in latitude. These observations indicate that the satellite moved in and out of the ducts in which the noise was trapped.

When VLF hiss is observed, the ionosphere is moderately disturbed. And the lower ionosphere is much more disturbed and moreover the collision frequency is

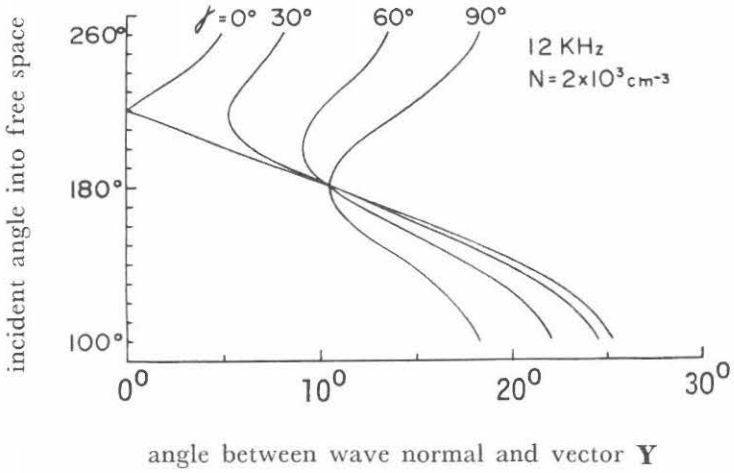

Fig. 23. Angle between the wave normal and the vector **Y** versus incident angle into free space as a parameter of γ, for the wave downcoming at 12 kHz. γ is the angle between the magnetic meridian plane and the incident plane. Electron density is 2×10^3cm^{-3}. Gyrofrequency is 1.08 MHz. The earth's magnetic field is at 10°32′ to the vertical. An incident angle more than 180° corresponds to a wave normal directed toward higher latitude.

higher. Thus, it will not be irrational to suppose that the field aligned irregularities (ducts) in which VLF hisses are trapped are formed above the auroral altitude (~1000 km). We adopt 2×10^3 cm^{-3} as the electron density at 1000 km altitude in the midnight of winter at auroral latitude, referring to the observational results given Brace et al. (1967).

On the other hand, we suggest that the energy of VLF hiss radiated three-dimentionally about the field line, is gradually focussed in the magnetic meridian plane as VLF hiss propagates downward in the magnetosphere and that VLF hiss propagates to an altitude (~1000 km) above auroral altitude in the field aligned duct with the wave normal nearly parallel to the field line.

It is found in Fig. 23 that a wave whose wave normal has a small angle to the field line propagates downward roughly within the magnetic meridian plane and penetrates into the free space with moderate angle of incidence toward higher latitude. Considering the results given in Fig. 23, our suggestion mentioned above is suitable for the explanation of the observed results on incident angles obtained with the CRT method and on the distribution of (R/L) values shown in Fig. 20 and Fig. 19 of part I, respectively.

Hence, we conclude that VLF hiss propagates downward in the field aligned duct to an altitude above auroral altitude and most of the energy comes down toward higher latitude roughly within the magnetic meridian plane and VLF hiss received on the ground has right-handed circular polarization and not so large an angle of incidence and that auroral hiss can not propagate to lower latitudes in the earth-ionosphere wave guide because of re-penetration into the auroral ionosphere and the inclination of incident angle toward higher latitude, so that auroral hiss is unique in the auroral zone and it is entirely different from low latitude type VLF hiss.

Acknowledgement

I wish to express my gratitude to the kind cooperation given by the wintering members of JARE 9 for the VLF observations at Syowa Station, Antarctica. Thanks are also due to Prof. A. Iwai for continuous encouragement and guidance and to my colleague for their useful discussions. I also wish to express my sincere thanks to Prof. H. Maeda of Geophysical Institute, Kyoto Univ. and Prof. I. Kimura of the Department of Electronics, Kyoto Univ., who kindly read the manuscript and made invaluable advice.

References

Brace L. H. et al. ; Global Ionospheric Behavior at 1000 km, J. G. R. **72**, 265, 1967.

Budden K. G. ; Radio Waves in the Ionosphere, Camb. Univ. Press 1961.

Clemmov P. C. & J. Heading ; Coupled forms of the differetial equations governing radio propagation in the ionosphere, Proc. Camb. Phil. Soc. **50**, 319, 1954.

Dowden R. L. ; Geomagnetic noise at 230 kHz, Nature **187**, 677, 1960.

Dowden R. L. ; Wide-band bursts of VLF radio noise (hiss) at Hobart, J. Aust. Phys. **65**, 114, 1962.

Ellis G. R. ; Low Frequency Electromagnetic Radiation associated with magnetic disturbances, P. S. S. **1**, 253, 1959.

Ellis G. R. ; Directional observations of 5 kc/s Radiation from the Earth's Outer Atmosphere, J. G. R. **65**, 839, 1960.

Gurnett D. A. ; A Satellite study of VLF hiss, J. G. R. **71**, 5599, 1966.

Harang L. & R. Larsen ; Radio Wave Emissions in the VLF band observed near the auroral zone-I Occurrence of emissions during disturbances, J. A. T. P. **27**, 481, 1965.

Harang L. & K. N. Hauge ; Radio Wave Emissions in the VLF band observed near the auroral zone-II Physical properties of the emissions, J.A. T. P. **27**, 499, 1965.

Harang L. ; VLF emission observed at stations close to the auroral zone and at stations on lower latitudes, J. A. T. P. **30**, 1143, 1968.

Hartz T. R. & N. M. Brice ; The General Pattern of Auroral Particle Precipitation, P. S. S.

15, 301, 1967.

Helms W. J & J. P. Turtle ; A cooperative report on the correlation between Aurorae, Magnetic, and ELF phenomena at Byrd Station, Tech. Rep. No. 3408 2 Stanford Univ. 1964.

Heyborne R. L. ; Observations of whistler-mode signals in the OGO Satellites from VLF ground station transmitters, Tech. Rep. No. 3415/3418-1 Radioscience Lab. Stanford Univ. 1966.

Hoffman R. A. & F. W. Berko ; Primary Electron influx to Dayside Auroral Oval, J. G. R. 76, 2967, 1971.

Holt O. & A. Omholt ; Auroral luminosity and absorption of cosmic radio noise, J. A. T. P. 24, 467, 1962.

Hower G. L. & W. I. Gluth ; Associations between VLF hiss and HF Radar Echoes from Field-Aligned Ionization, J. G. R. 70, 649, 1965.

Iwai A. et al. ; The observation of VLF emissions at Moshiri, Proc. Res. Inst. Atmospherics Nagoya Univ. 11, 29, 1964.

Iwai A. & Y. Tanaka ; Measurement of polarization, incidend angle and direction of VLF emissions-(I), Pro. Res. Inst. Atmospherics Nagoya Univ. 15, 1, 1968.

Jespersen M. et al. ; pp 27 'Electron density profiles in ionosphere and exosphere' North-Holland Pub. Company 1966.

Jörgensen T. S. ; Some observations of VLF hiss and correlated phenomena, J. A. T. P. 26, 626, 1964.

Jörgensen T. S. ; Morphology of VLF hiss zones and their correlation with Particle Precipitation Events, J. G. R. 71, 1367, 1966.

Jörgensen T. S. ; Interpretation of auroral hiss measured on OGO 2 and at Byrd Station in terms of incoherent Cerenkov radiation, J. G. R. 73, 1055, 1968.

Kuck G. A. ; Local time dependence of aurora zone electron spectra, Ann. Geophys. 26, 689, 1970.

Laaspere T. et al. ; Observations of Auroral Hiss, LHR Noise, and other phenomena in the frequency range 20Hz-540kHz on OGO 6, J. G. R. 76, 4477, 1971.

Lund et al. ; Electron number densities in auroral irregularities : Comparison of Backscatter and Satellite Data, J. G. R. 72, 1053. 1967.

Maeda K. & I. Kimura ; A Theoretical Investigation on the propagation path of the Whistling Atmospherics, Rep. Ionos. Res. Japan 5, 105, 1956.

Martin L. H. et al. ; Association between aurorae and VLF hiss observed at Byrd Station, Antarctica, Nature 187, 751, 1960.

Morozumi H. M. ; Diurnal variation of aurora zone geophysical disturbances, Rep. Ionos. Space Res. Japan 19, 286, 1965.

Morozumi H. M. & R. A. Helliwell ; A correlating study of the diurnal variation of upper atmospheric phenomena in the southern auroral zone, Sci. Rep. No. 2 Radioscience Lab. Stanford Univ. 1966.

Mosier S. R. & D. A. Gurnett ; VLF Measurement of the Poynting Flux along the Geomagnetic Field with the Injun 5 Satellite, J. G. R. 74, 5675, 1969.

Pitteway M. L. V. & J. L. Jespersen ; A numerical study of the excitation, internal reflection and limiting polarization of whistler waves in the lower ionosphere. J. A. T. P. 28, 17, 1966.

Tanaka Y. & M. Kashiwagi ; Correlation between VLF hiss and geomagnetic activity in

Hokkaido, Proc. Res. Inst. Atmospherics Nagoya Univ. **15**, 67, 1968.

Tanaka Y. et. al. ; VLF hiss at Syowa Station, Antarctica, Proc. Res. Inst. Atmospherics Nagoya Univ. **17**, 43, 1970.

Vershinin E. F. ; About the intensity of the hiss near inner boundary of the plasmapause and about the bursts of hiss with drifting frequency, Ann. Geophys. **26**, 703, 1970.